Morphology and Evolution of Herbig Ae disks

E. Di Folco[1], A. Dutrey[2], J. Olofsson[3], S. Guilloteau[2], S. Wolf[4]

1/Laboratoire AIM, CEA-Saclay/Uni.Paris7/CNRS, France, 2/LAB-OASU, Bordeaux, France
3/MPIA Heidelberg, Germany, 4/Universität Kiel, Germany

We used VLTI/MIDI to resolve few famous Herbig Ae disks (AB Aurigae, MWC758, HD97048) to characterize the morphology of their 2-10 AU inner disks. Radiative transfer modelling allows us to determine the flaring index and the scale height, taking advantage of the synergy between interferometric and spectro-photometric quantities. Radial variations of the dust properties (grain growth and crystallization) can also be detected. In connection with earlier sub-mm interferometric studies, the disk morphology is quasi-continuously determined on spatial scales ranging from 2 to few 100 AU, and is compared with theoretical models. We focus here on the comparison between the inner (2-10AU) and outer (50-250AU) regions of the flared disk surrounding MWC758.

MWC758 Observations: the 8-32 μm spectrum

Mineralogy from Spitzer IRS spectrum

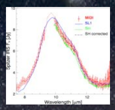

MIDI vs. IRS

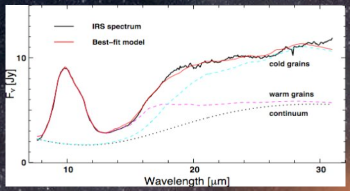

Dust abundance (mass fractions)

	Warm Component				Cold Component			
Grain Temperature (T_{gr})		283 K				95 K		
Dust species / Grain size	0.1 μm	1.5 μm	6 μm	Total	0.1 μm	1.5 μm	6 μm	Total
Amorphous Olivine (%)	56.3 ± 2.7	7.2 ± 0.8	4.5 ± 0.4	68	–	4.1 ± 0.9	–	4
Amorphous Pyroxene (%)	7.0 ± 1.3	12.5 ± 1.0	0.3	20	59.5 ± 2.8	17.0 ± 0.9	6.0 ± 0.4	83
Amorphous Silica (%)	–	–	2.1 ± 0.4	2	–	–	–	–
Forsterite (%)	2.1 ± 0.5	–	–	2	0.4	–	–	–
Enstatite (%)	0.3	2.8 ± 0.6	4.9 ± 1.5	8	0.9 ± 2.1	–	12.1 ± 0.6	13
Total (all species) (%)	65.7	22.5	11.8		60.8	21.1	18.1	
Amorphous Si (%)		90				87		
Crystalline Si (%)		10				13		

We modeled the IRS spectrum with a warm and a cold independent dust populations, and determined a **maximum crystallinity of 15%** for each. The fraction of large grains is slightly larger than in the ISM distribution. The abundances of forsterite, enstatite and silica are consistent with model predictions, where crystalline species are produced in the hot inner disk through thermal annealing and then redistributed in the upper layers and outer disk via radial and vertical mixing (Gail 2004, Shu 1994).

Inner vs. Outer disk dust emissivity

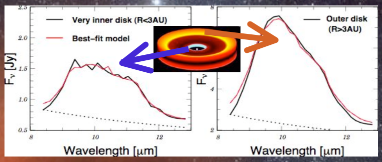

The **correlated flux** at long baseline (B>70m) approximates the spectrum of the unresolved, inner rim region (<2AU): $F_{corr} = F(\lambda) \times Vis(\lambda)$. The outer disk spectrum (>2AU) is estimated by subtracting this quantity to the total source flux (van Boeckel et al 2004). Evidences are found for a **change of dust emissivity in the very inner, hot disk**. Our modeling shows that an increase of the crystallinity abundance by a factor 2 to 3 in the most central region could account for the observed discrepancy.

MWC758 interferometric observations

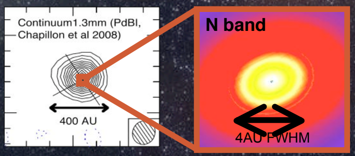

VLTI-MIDI observations

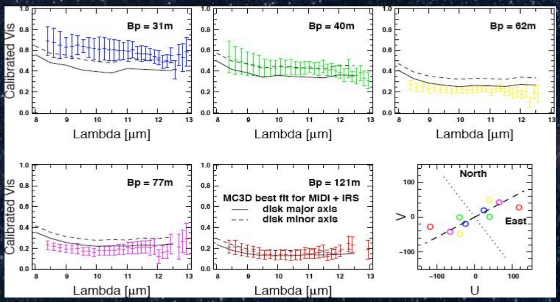

Radiative Transfer modeling with MC3D

We consider a passive disk, with a parmeterized description of the density, leaving the flaring index (β) and the scale height (h_0 at 100AU) as the only free parameters. Inner and outer radii, as well as disk inclination, orientation and mass are provided by earlier observational constraints (Eisner2004, Chapillon2008, Isella2008). The dust temperature is self-consistently calculated by the 2D radiative transfer code MC3D (Wolf 1999,2001).

$$\rho(r,z) = \rho_0 \left(\frac{r}{r_0}\right)^{-\alpha} \exp\left\{-\frac{1}{2}\left[\frac{z}{h(r)}\right]^2\right\}$$

$$h(r) = h_0 \left(\frac{r}{r_0}\right)^{\beta}$$

Thermal and scattered emissions from the grains of the disk atmosphere are taken into account to produce the SED and spectrally dispersed visibilities. The combination of the SED and Vis-fit alleviates the intrinsic degeneracies, since they constrain the total emission and its radial profile together.

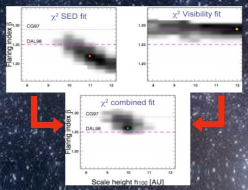

Inner vs. Outer disk characteristics (mid-IR vs. mm)

	Inner disk (2-10 AU)	Outer disk (>50 AU)
Flaring index	β = 1.26	β = 1.3
Scale height (@100AU)	h_0 = 10 ± 0.5 AU	h_0 ~ 8 AU
Grains	Moderate signs of grain growth and crystallization	Evidence for grain growth
Gas	-	CO depletion (x100)

Conclusions

- **Morphology**: the flaring index and the scale height confirm Meeus (2001) classification, and present a good agreement with the outer disk flared structure revealed by the PdBI. Consistently smaller than AB Aur disk at IR and mm wavelengths (Pietu 2005, Di Fiolco 2009). The inner rim constibutes to about 20% of the total flux in the N-band.
- **Mineralogy**: the IRS spectrum is dominated by sub-micron, amorphous silicates, but shows in addition signs of grain evolution with a moderate abundance of crystalline grains (10-15%, mostly Mg-rich crystals: forsterite and enstatite). We also find a larger contribution of large grains compared to the ISM distribution.
- **Evolution status**: moderate signs of grain evolution (growth and crystallization) are found in the dust properties of the inner and outer disks, but the gaseous component presents in contrast a clear CO-depletion, which suggests that the outer disk is already more significantly evolved than the central regions.

References:

Chapillon et al., 2008, A&A, 488, 565

Chiang & Goldreich, 1997, ApJ, 490, 368

D'Alessio et al. 1998, ApjJ, 500, 41

Di Folco et al. 2009, A&A , 500, 106

Dullemond et al., 2001, ApJ, 560, 957

Eisner et al. 2004, ApJ, 613, 1049

Gail 2004, A&A, 413, 571

Isella et al. 2008, A&A, 483, L13

Meeus et al. 2001,A&A, 365, 476

Piétu et al., 2005 A&A, 443, 945

van Boeckel et al., 2004, Nature, 432, 479

Wolf et al., 1999, A&A, 349, 839